JOURNAL OF SPACECRAFT AND ROCKETS
Vol. 36, No. 5, September–October 1999

Application of the 1998 Version of the Aeroprediction Code

F. G. Moore,* R. M. McInville,† and T. C. Hymer‡
U.S. Naval Surface Warfare Center, Dahlgren, Virginia 22448-5100

The U.S. Naval Surface Warfare Center aeroprediction code has been extended to the roll position of 45 deg (fins in "×" or cross-roll orientation) in addition to the roll position of 0 deg (fins in "+" or plus-roll orientation). It has also been extended to compute aerodynamics of nonaxisymmetric bodies based on an equivalent axisymmetric body. In addition, the nonlinear aerodynamic loads have been distributed over the body and lifting surfaces to provide a more useful tool for preliminary structural analysis. Finally, new technology was developed to improve the prediction of axial force at angle of attack. These new technologies have been integrated into the 1995 Aeroprediction Code (AP95) and will be transitioned to legitimate users as the 1998 Aeroprediction Code (AP98). To make the AP98 more user friendly, an upgraded pre- and postprocessing, personal-computer interface was also developed. The theoretical methods of the AP98 are summarized, and a sample is shown of the comparisons of the AP98 predictions of static aerodynamics for several missile configurations to experimental data. Comparisons of theory and experiment show that the AP98, on average, is at least as good as the AP95 and, in general, may be slightly better.

Nomenclature

a, b	= semimajor and semiminor axes, respectively, of ellipse
b	= wing span (not including body), ft
C_A	= axial-force coefficient
C_L	= lift coefficient
C_{ℓ_P}	= roll-damping moment coefficient
C_M	= pitching-moment coefficient (based on reference area and body diameter if body present, or mean aerodynamic chord if wing alone)
$C_{M_q} + C_{M_\alpha}$	= pitch-damping moment coefficient
C_N	= normal-force coefficient
C_{N_B}	= normal-force coefficient of body alone
$C_{N_{B(W)}}, C_{N_{B(T)}}$	= normal-force coefficient on body in presence of wing or tail
$C_{N_{T(V)}}$	= negative normal-force coefficient component on tail due to wing or canard-shed vortex
$C_{N_{W(B)}}, C_{N_{T(B)}}$	= normal-force coefficient of wing or tail in presence of body
C_{N_α}	= normal-force coefficient derivative
$C_{n_{P_\alpha}}$	= magnus moment coefficient derivative
k, k_1	= parameters used to define corner radius for squares and triangles, $k = r_n/W_m$; $k_1 = r_n/W$
ℓ	= body length
M_∞	= freestream Mach number
r	= local body radius, ft
r_n	= corner radius of a rounded corner on square or triangle
W, W_m	= diameter and maximum diameter, respectively, of a triangle or square as measured normal to the velocity vector
x, y, z	= axis system fixed with x along centerline of body, y out right wing when viewed from rear
α	= angle of attack, deg
δ_W, δ_T	= deflection of wing or tail surfaces (deg), positive leading edge up
Φ	= roll position of missile fins: $\Phi = 0$ deg corresponds to fins in the plus (+) orientation; $\Phi = 45$ deg corresponds to fins rolled to the cross (×) orientation

Received 1 May 1998; revision received 29 December 1998; accepted for publication 29 January 1999. This paper is declared a work of the U.S. Government and is not subject to copyright protection in the United States.

*Senior Aerodynamicist, Weapons Systems Department, Dahlgren Division. Associate Fellow AIAA.

†Aerospace Engineer, Weapons Integration Branch, Weapons Systems Department, Dahlgren Division.

‡Aerospace Engineer, Systems Engineering Branch, Weapons Systems Department, Dahlgren Division.

Introduction

THE U.S. Naval Surface Warfare Center Aeroprediction Code (APC) has been developed from its inception in 1972 (Ref. 1) to the present time with a primary objective. This objective is to provide the aerodynamicist with a set of reasonably accurate aerodynamics in a cost effective and timely manner. The original application uses of the earlier versions of the APC [AP72 (Ref. 1), AP74 (Ref. 2), AP77 (Ref. 3), and AP81 (Ref. 4)] were to provide inputs to particle-ballistic or trim-performance models and to be used in aerodynamic design optimization. As weapons flew faster and to higher angles of attack (AOA), the code application uses included convective heat transfer inputs [AP93 (Ref. 5) and AP95 (Ref. 6)] and, more recently, nonlinear loads for structural beam analysis [AP98 (Ref. 7)]. During the development of the APC over the past 27 years, many new technologies[1–21] have been developed to meet the ever-changing flight requirements. These flight requirements include Mach numbers 0–15, AOAs to 90 deg, control deflections of 0 to ±30 deg, trim roll orientation of 0 or 45 deg (fins in + or × roll orientations, respectively), and body geometry that is axisymmetric or asymmetric.

The objective, application uses, and requirements for the AP98 are as follows: The objective for APC is to predict aerodynamics cost effectively and with reasonable accuracy over the flight envelope of interest to weapons designers. The application requirements of APC are as follows: 1) inputs to three-degree-of-freedom/trim performance models, 2) aerodynamic design (preliminary), 3) preliminary structural loadings, and 4) convective heat transfer inputs.

The overall flight requirements for APC are as follows: Mach number, 0–15; AOA, 0–90 deg; control deflection, ±30 deg; roll orientation, 0 and 45 deg; sets of fins, 0, 1, 2 required, 3 desired; and body geometry, axisymmetric required, nonaxisymmetric treatment desired. Table 1 summarizes the evolution of the APC development. Figure 1 shows the general outline of the axisymmetric body configurations for which the code is applicable, and Fig. 2 shows the cross sections of the various nonaxisymmetric bodies for which the AP98 can be used.

The latest version of the APC released to the public AP95 (Ref. 6) has several limitations when viewed against the overall requirements. First, the code is limited to the roll position of $\Phi = 0$ deg aerodynamics. Because the code is a semi-empirical model used for preliminary design, it is important that aerodynamics be available in the roll position of $\Phi = 45$ deg as well. This new technology was therefore developed[16] and will be a part of the AP98. Second, although the AP95 defined nonlinear aerodynamic loads to AOA of

Table 1 Evolution of APC

Version	Weapons	Flight conditions				
		Aerodynamics	Mach number	AOA range	Roll	Computers
1972	Unguided projectiles	C_A, C_N, X_{CP}	0–3	0–15 deg	$\Phi = 0$ deg	CDC
1974	Missiles, projectiles, rockets	C_A, C_N, X_{CP}	0–3	Same	Same	CDC
1977	Missiles, projectiles, rockets	C_A, C_N, X_{CP}, C_{ℓ_p}, $C_{M_q} + C_{M_{\dot{\alpha}}}$, $C_{n_{P\alpha}}$	0–3	Same	Same	CDC, IBM
1981	Missiles, projectiles, rockets	Same	0–8	0–15 deg (limited conf. at higher α)	Same	CDC, IBM, VAX
1993	Missiles, projectiles, rockets	Same	0–20	0–30 deg	Same	CDC, IBM, VAX, Silicon Graphics
1995	Missiles, projectiles, rockets	Same	Same	0–90 deg	Same	Interactive PC
1998	Same (asymmetric body treatment)	Same	Same	Same	$\Phi = 0$, 45 deg	Interactive PC

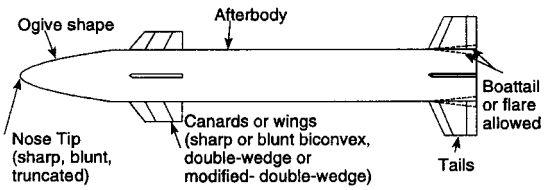

Fig. 1 Typical axisymmetric weapon-configuration geometry requirements.

90 deg, it did not distribute all of these loads over the body and lifting surfaces to make the code more useful to the structural engineer who might be using the code to perform a beam analysis of a missile structure. This problem was also addressed and documented in Ref. 18.

A third problem that existed with the AP95 was the accuracy of the axial-force coefficient at high AOA. This problem became more prominent at subsonic Mach numbers where the axial force could go negative, and at all Mach numbers when a control deflection was of sign opposite to the AOA. New technology was developed[19] to correct this problem, and this new technology will also be a part of the AP98. The final weakness of the AP95 compared to the aero-prediction requirements is the limitation of axisymmetric bodies. This was an extremely difficult problem to solve. However, after a couple of years where several difficult technology shortfalls were overcome, this limitation was also removed, and documentation on the new technology was just completed.[21]

The purpose of this paper is thus threefold. First, the technology that will be a part of the AP98 will be briefly summarized. Whereas Refs. 1–21 summarize each new technology and the evolution of the APC, this is the first external paper that summarizes all of the methods of the AP98. Second, several example cases will be shown where the robustness and accuracy of the AP98 compared to the AP95 will be illustrated by comparing to experimental data. Finally, some thoughts on the future direction of the APC development will be given.

Summary of Theoretical Methodology

The theoretical methodology will be discussed in terms of the low-AOA methods developed for the AP81 and prior versions of the APC and the newer high-Mach-number, high-AOA methods developed for the AP93, and more recent versions. The methods developed since the AP95 will be briefly discussed on an individual basis. No details of any of the theoretical approaches will be given, as they are all well documented in Refs. 1–21.

Low-AOA Methods (AP72, AP74, AP77, and AP81)

To the authors' knowledge the AP72 was the first total force and moment APC. It computed body-alone aerodynamics over the Mach number range 0–2.5 and AOA to about 10 to 15 deg. The most difficult coefficient to compute was the axial force. This difficulty was primarily a result of the fact that the nose could be sharp, blunted, or truncated (Fig. 1). To get an accurate axial force, new technology was developed[1] where the modified Newtonian theory (MNT) was combined with the second-order perturbation theory of Van Dyke.[22] This second-order accuracy in wave drag prediction was extended in Mach number[4] to values as high as 8 by making improvements[9] to the second-order shock-expansion theory (SOSET).[23] For transonic Mach numbers and below, numerical techniques[10,24] in combination with empiricism and table look-up were employed. Skin-friction drag was calculated by the method of Van Driest.[25] Base drag and rotating band drag were calculated empirically based on an average of wind-tunnel measurements.[1] Lift of the body alone was predicted by the method of Tsien,[26] Wu and Aoyoma,[24] or DeJarnette et al.[9]

Two sets of lifting surfaces were added to the body in the AP74 Ref. 2 (Fig. 1). Perturbation methods were used for both the wing-alone normal and axial-force predictions. To account for the blunt leading and trailing edges of the wing, MNT and empirical estimates, respectively, were used for axial-force information. Again, Van Driest II was used for the wing skin-friction computations. Wing-body interference was calculated by modifying the slender body and linear theory methods of Ref. 27 so that nonslender configurations could be considered.

Dynamic derivatives (pitch damping and roll damping) were added to the aerodynamic prediction capability in 1977 (Ref. 3). The low-AOA versions of the APC could be used with reasonable confidence up to about 10-deg AOA. Predictions became increasingly inaccurate as AOA increased above about 10 deg.

High-Mach-Number and Moderate-AOA Methods (AP93)

The linear theory methods of the AP81 and prior versions were simply unacceptable for predicting nonlinear aerodynamics on configurations at moderate to high AOA. As a result, new technology[5,11–14] was developed to extend the AOA and Mach number capability of the AP81. The approach used for extending the Mach number was to extend the SOSET to include real gas effects.[11] This extended theory then allowed more accurate inviscid surface temperatures to be computed. This in turn allowed the convective heat transfer to be predicted,[13] with engineering accuracy, at all Mach numbers of interest along and around the body. To account for base-drag nonlinearities, new wind-tunnel data were taken, and the base-drag AOA model refined.[14]

A new approach was developed to account for nonlinearities in normal force and center-of-pressure properties at moderate to high AOA. Basically, this approach utilized several large missile component databases in conjunction with the low-AOA linear theory methods of the AP81. The total normal-force coefficient of a wing-body-tail configuration was written in a form similar to that of Ref. 27, that is,

$$C_N = C_{N_B} + C_{N_{W(B)}} + C_{N_{B(W)}} + C_{N_{T(B)}} + C_{N_{B(T)}} + C_{N_{T(V)}} \quad (1)$$

Each term of Eq. (1) was then broken down into a linear and nonlinear component. The linear term was estimated based on the linear theory methods of Ref. 4. The nonlinear terms of the body-alone normal force and center of pressure were predicted by modifications to the Allen–Perkins Viscous Crossflow Theory.[28] The other nonlinear terms of Eq. (1) were calculated in conjunction with the data bases[29–31] and Ref. 4. Then, analytical approximations or tables were used to predict each nonlinearity. The method was then checked out on the wind-tunnel databases from which the nonlinearities were developed and fine tuned based on other missile configuration databases. This approach, which the author calls the direct

Table 2 AP98 methods for body-alone aerodynamics

Component/Mach number region	Subsonic, $M_\infty < 0.8$	Transonic, $0.8 \le M_\infty \le 1.2$	Low supersonic, $1.2 \le M_\infty \le 1.8$	Mod/high supersonic, $1.8 \le M_\infty \le 6.0$	Hypersonic, $M_\infty > 6.0$
Nose wave drag	Empirical[1]	Semi-empirical based on Euler solutions[4]	Second-order Van Dyke Plus MNT[1]	SOSET plus IMNT[9]	SOSET plus IMNT[9] modified for real gases[11]
Boattail or flare wave drag	——	Wu and Aoyoma[1]	Second-order Van Dyke[22]	SOSET[23]	SOSET for real gases[11]
Skin-friction drag			Van Driest II[25]		
Base drag			Improved empirical method[14]		
Axial force at α			Improved empirical method[19]		
Aeroheating information		——		SOSET plus IMNT for real gases[13]	
Inviscid lift and pitching moment	Empirical[1]	Semi-empirical based on Euler solutions[4]	Tsien first-order crossflow[26]	SOSET[23]	SOSET for real gases[11]
Viscous lift and pitching moment			Improved Allen and Perkins crossflow[31]		
Nonaxisymmetric body aerodynamics ($\Phi = 0, 45$ deg)			Modified Jorgensen[21,32]		
Nonlinear structural loads available ($\Phi = 0, 45$ deg)		No		Yes[18]	

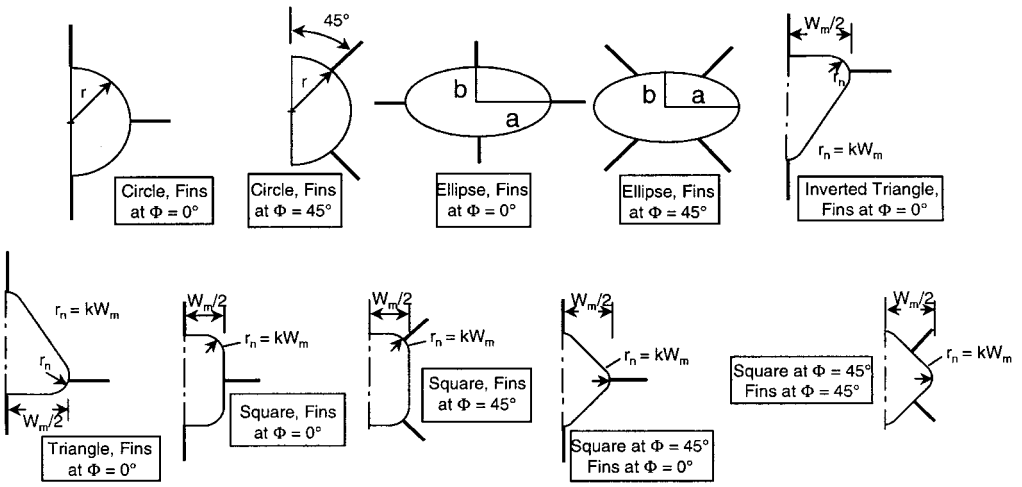

Fig. 2 Some noncircular cross-section, wing-body configurations of interest.

approach (because of direct usage of wind-tunnel data to approximate each nonlinearity), was found to give average accuracy levels on normal-force coefficient of ±10% and center of pressure ±4% of body length for AOA to 30 deg. The major reason for the limitation to 30-deg AOA was because the wing-alone lift was approximated by a second-order equation in AOA. Also, the data in the large data bases[29–31] were used only up to AOA of 30 deg in the development of the tables to approximate the nonlinearities in each of the terms in Eq. (1). Also, only the roll position of $\Phi = 0$ deg was considered in the methodology.

High-AOA and Asymmetric Body Methods (AP95 and AP98)

Many missiles fly above 30-deg AOA during their launch or terminal phases. As a result, new technology was developed to extend the AOA capability in the $\Phi = 0$ deg roll to 90-deg AOA.[6,15] This high-AOA technology was then extended to the roll position of $\Phi = 45$ deg (Refs. 16, 17, and 19). All of these nonlinear loads were then distributed over the body and lifting surfaces using a Navier–Stokes code to aid in the methodology development process.[18] Finally, the constraint of axisymmetric bodies was eliminated with development of a robust method for noncircular cross-section missile configurations.[21] Tables 2–4 summarize the various theoretical methods that will be a part of the AP98 (Refs. 1–4, 6, 9, 11, 13, 14, 16, 18, 19, 21–23, 25, 26, 31–34).

The AP95 and AP98 were the first versions of the APC to be converted to a personal computer format with an interactive pre- and postprocessing software package as part of the APC transition. The preprocessing part of the software package has automated many geometry inputs, which decreases the input time from as much as 4 h to as little as 5 to 10 min. The postprocessing software has many automated plots as well as tables of data again to reduce time involved and improve productivity. An experienced user of the APC can now get a complete set of aerodynamics in less than 15 min from input to output. The AP98 is currently in operation on a personal computer with Microsoft Windows 95 software and an Intel 200-MHZ chip. Aerodynamics for 200 cases (one case is one configuration, one AOA, and one Mach number) can be obtained in less than 1 min of execution time on the personal computer. This is the same execution time taken for a single case on the mainframe computer at the U.S. Naval Surface Warfare Center, Dahlgren Division (NSWCDD), for the first version of the code AP72, which considered only body-alone cases. In other words during the 27-year history of the APC code development, the computational cost for a set of approximate aerodynamics has gone down by several orders of magnitude. Also, the time it takes to get this set of aerodynamics has been reduced by approximately two orders of magnitude. The combination of the productivity improvements, enhanced capability, and improved accuracy levels is the major reason the AP95 has been transitioned to 139 users around the world.

Table 3 AP98 methods for wing-alone and interference aerodynamics

Component/Mach number region	Subsonic, $M_\infty < 0.8$	Transonic, $0.8 \le M_\infty \le 1.2$	Low supersonic, $1.2 \le M_\infty \le 1.8$	Mod/high supersonic, $1.8 \le M_\infty \le 6.0$	Hypersonic, $M_\infty > 6.0$
Wave drag	——	Empirical[2]	Linear theory plus MNT[2]	Shock expansion (SE) plus MNT along strips[9]	SE plus MNT for real gases along strips[9]
Skin-friction drag			Van Driest II[25]		
Trailing-edge separation drag			Empirical[2]		
Body-base pressure caused by tail fins			Improved empirical[14]		
Inviscid lift and pitching moment					
Linear	Lifting surface theory[2]	Empirical[2]	3-D Thin Wing Theory (3DTWT)[2]	3DTWT or SE[2,9]	3DTWT or SE[2,11]
Nonlinear			Empirical[6,16]		
Wing-body, body-wing interference ($\Phi = 0, 45$ deg)					
Linear			Slender body theory or linear theory modified for short afterbodies[6,16]		
Nonlinear					
Wing-body, interference due to δ ($\Phi = 0, 45$ deg)					
Linear			Slender body theory[16]		
Nonlinear			Empirical[6,16]		
Wing-tail interference ($\Phi = 0, 45$ deg)			Line vortex theory with modifications for $K_{W(B)}$ term and nonlinearities[16]		
Aeroheating		None present		SE plus MNT[13]	SE plus MNT real gases[13]
Nonaxisymmetric body aerodynamics ($\Phi = 0, 45$ deg)			Improved Nelson, EST[21,33,34]		
Nonlinear structural loads available ($\Phi = 0, 45$ deg)		No		Yes[18]	

Table 4 AP98 methods for dynamic derivatives[3]

Component/Mach number region	Subsonic, $M_\infty < 0.8$	Transonic, $0.8 \le M_\infty \le 1.2$	Low supersonic, $1.2 \le M_\infty \le 1.8$	Mod/high supersonic, $1.8 \le M_\infty \le 6.0$	Hypersonic, $M_\infty > 6.0$
Body alone			Empirical		
Wing and interference roll-damping moment	Lifting surface theory	Empirical	Linear thin-wing theory	Linear thin-wing or strip theory	
Wing magnus moment			Assumed zero		
Wing and interference pitch-damping moment	Lifting surface theory	Empirical	Linear thin-wing theory	Linear thin-wing or strip theory	

Application Examples

Several cases are selected to show the comparison of the AP98 aerodynamic computations to those of the AP95 and experimental data. The cases selected are chosen not only to show the accuracy levels of the AP98, but its robustness in terms of weapon configurations and flight conditions as well. A total of 13 examples were given in Ref. 7, but only seven of those examples will be shown here because of space considerations. The interested reader is referred to this reference for more details of the comparisons of the AP95 to experiment and other theoretical methods. In general, we found that the AP98 gave slightly better normal-force and axial-force predictions than the AP95 in the $\Phi = 0$ deg roll plane. However, the AP95 gave slightly better pitching-moment predictions (and hence center of pressure) on some configurations than the AP98 in the $\Phi = 0$ deg roll plane. The reason for this poorer prediction of pitching moment by the AP98 on some configurations will be discussed as part of the Fig. 3 discussion. On the other hand, the AP98 gave aerodynamics for the $\Phi = 45$ deg roll plane, which were at least as good as, if not better than, $\Phi = 0$ deg. The AP98 also gave aerodynamics for nonaxisymmetric body cases, as well as distributed nonlinear loads.

The first case considered is a wing-body-tail configuration with experimental data given in Ref. 35. The configuration is shown in Fig. 3a, and data were available for both wing- and tail-control options. This configuration has a length of about 18 calibers with a tangent ogive nose 2.25 calibers in length. It has wings and tails of fairly high aspect ratios of 2.8 and 2.6, respectively. Data were taken at Mach numbers 1.5 to 4.63 for AOAs to 45 deg and control deflections of 0 and 10 deg at M of 1.5 and 2.0 and 0 to 20 deg at M of 2.35 to 4.63. The data were taken at a Reynolds number of 2.5×10^6/ft, and boundary-layer trips were also used. The model has a hollow chamber, and chamber axial-force measurements were given separately in Ref. 20. These results were added to the

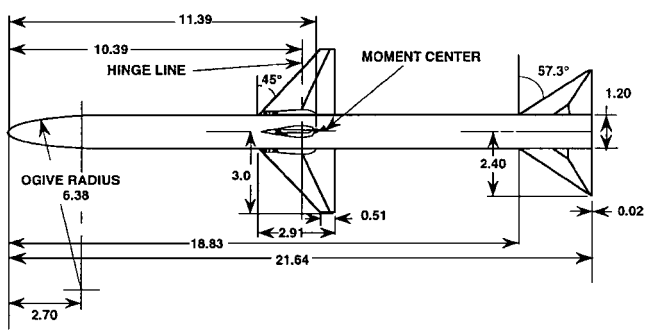

Fig. 3a Wing-body-tail configuration used in validation process.[35]

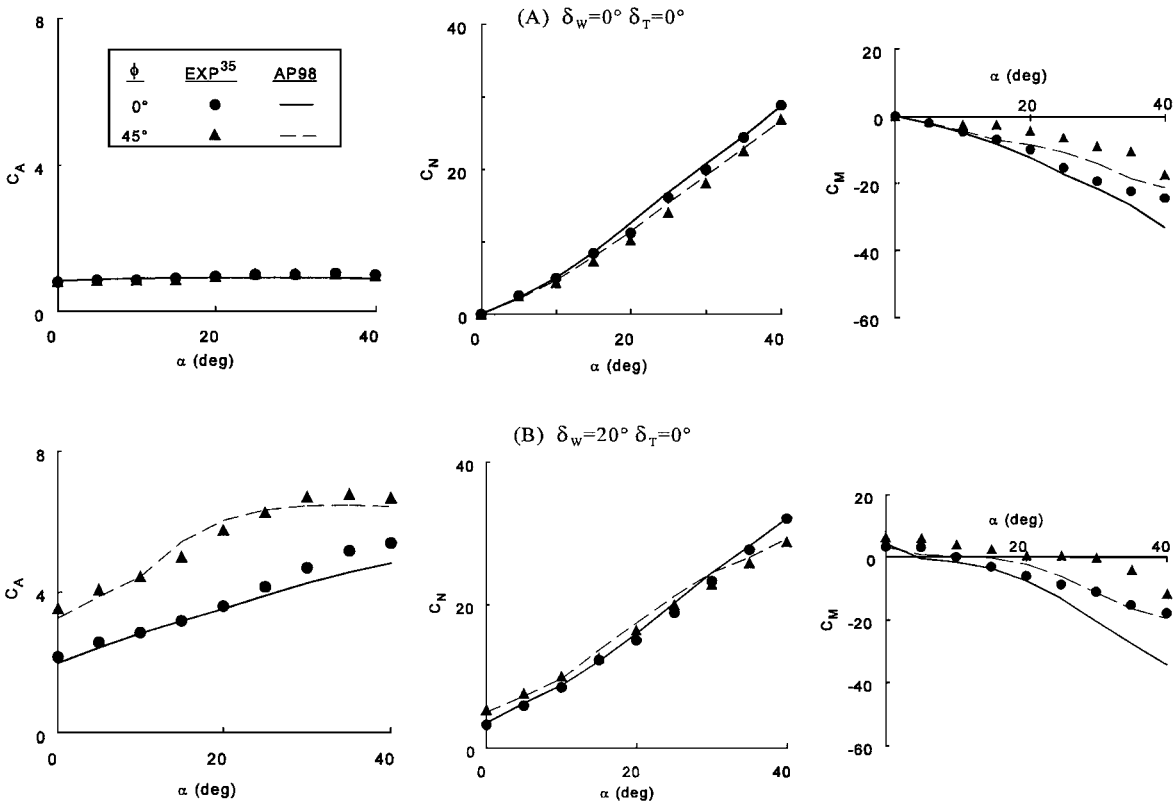

Fig. 3b Axial-, normal-, and pitching-moment coefficient comparisons of theory and experiment ($M_\infty = 2.87$).

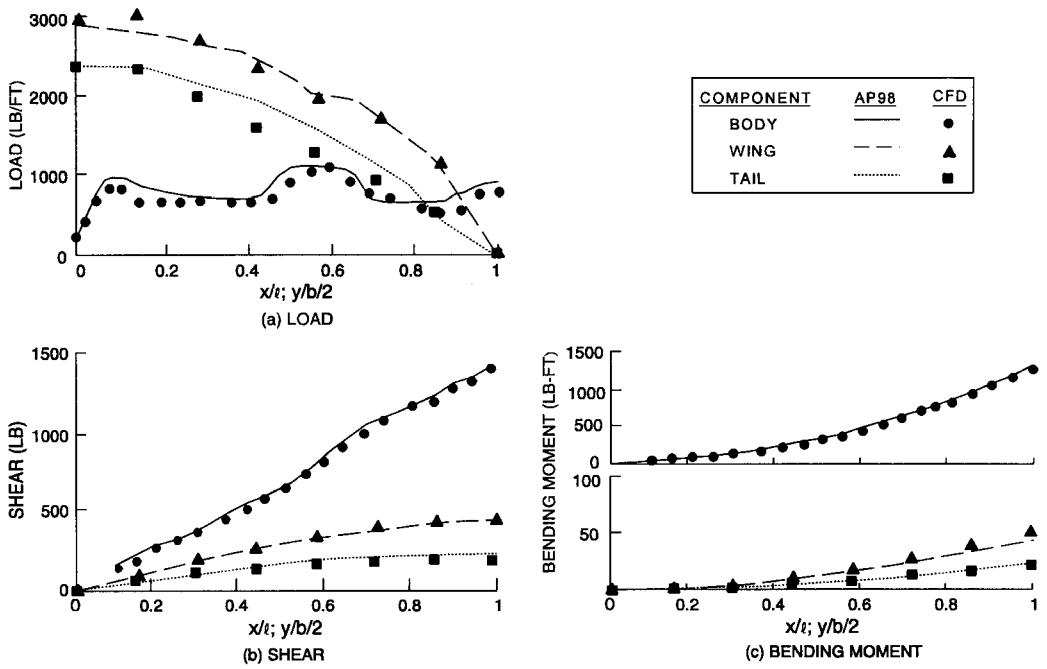

Fig. 3c Load, shear, and bending moment for configuration of Fig. 3a ($M_\infty = 2.87$, $\Phi = 0$ deg, $\alpha = 40$ deg).

forebody axial-force measurements to compare with the AP95 and AP98.

Figure 3b presents the results of C_A, C_N, and C_M for $M_\infty = 2.87$, where the AP98 is compared to experiment as a function of AOA for the roll positions of 0 and 45 deg and for wing-control deflection of 0 and 20 deg. As seen in the Fig. 3b, the AP98 gives very good agreement with experimental data and is well within the average accuracy goals of ±10% on C_A and C_N and ±4% of body length on center of pressure. Notice that the pitching-moment comparisons to data degrade above AOA of 20 deg, which is believed to be because of the internal shock interactions of the bow shock onto the wing and the wing shock onto the tail. This interaction is not explicitly accounted for in the AP98. Even with this discrepancy the worst case center-of-pressure error occurs for $\Phi = 0$ and AOA = 40 deg. For this case the error in center of pressure is still just over 3% of the body length, and the average center of pressure over the AOA range of 5–40 deg is less than that. Both of these numbers are within the ±4% goal of the AP98.

Figure 3c illustrates the new nonlinear structural load capability of the AP98. Shown in the figure is local load, shear, and bending moment as a function of x/l for the body and $y/(b/2)$ for the wing and tail. The AP98 results are compared to a Navier–Stokes

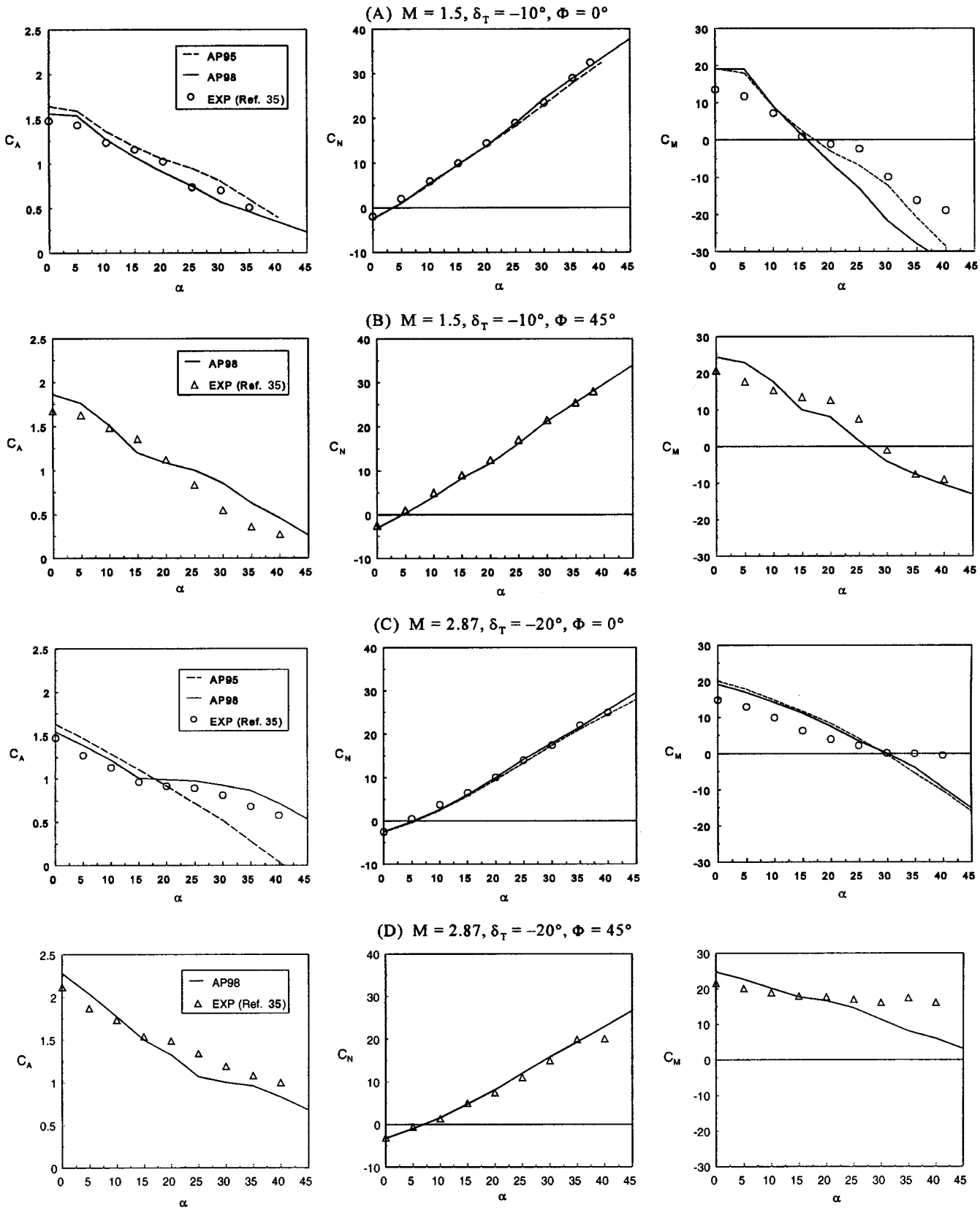

Fig. 3d Comparison of experiment and theory for C_A, C_N, and C_M for Fig. 3a tail-control case.

calculation.[18] Note the excellent agreement of the local load, shear, and bending moment between the AP98 and Navier–Stokes computations on the body, wings, and tails. The particular case shown is the $\Phi = 0$ deg and $\alpha = 40$ deg case of Fig. 3b.

Figure 3d presents the tail-control comparisons of theory and experiment for the Fig. 3a configuration. These figures illustrate both the $\Phi = 0$ and 45 deg aerodynamic computations at $M = 1.5$, 2.87, and 4.6 for the AP95 and AP98. Control deflections of $\delta_T = -10$ for $M = 1.5$ and $\delta_T = -20$ for Mach 2.87 and 4.6 are shown. Of course, the AP95 results are only shown for the $\Phi = 0$ deg plane. Several points are worthy of note. First, both the AP95 and AP98 give good agreement to experiment on normal force. The AP98 gives good agreement to axial force at all conditions, whereas the AP95 deviates from data at high AOA for this case where α and δ are opposite in sign. Third, the internal shock interactions increase in strength as Mach number and AOA increase. Eventually, as AOA

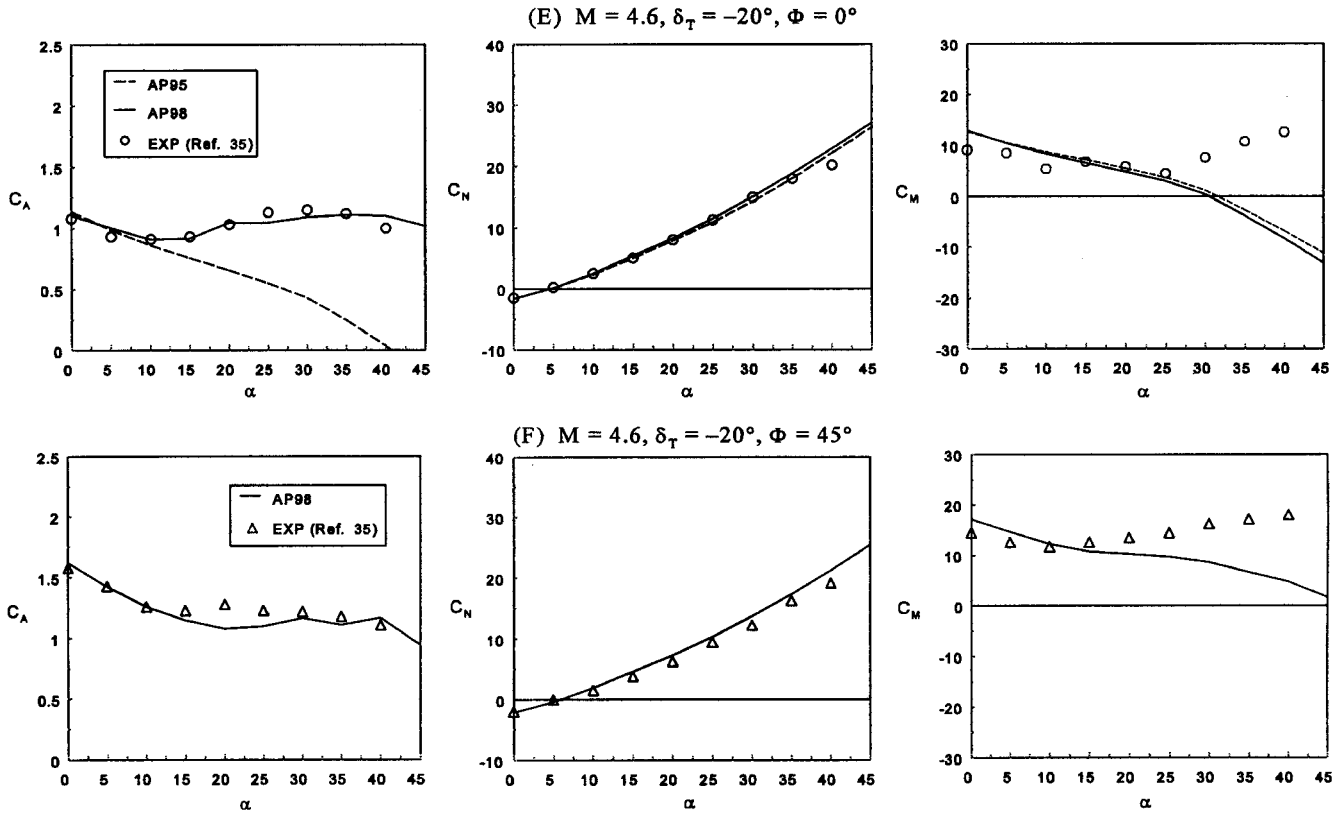

Fig. 3d Comparison of experiment and theory for C_A, C_N, and C_M for Fig. 3a tail-control case (continued).

gets higher, this discrepancy goes away (not shown). At the worst-case condition the AP98 still meets the ±4% of body length goal on center-of-pressure error, however.

The final point to be made on Fig. 3d is the fact that at $\Phi = 0$ deg roll and $M = 1.5$ the AP95 gives better comparisons of pitching-moment data than the AP98 in the angle-of-attack range from 15 to 45 deg. The reason the AP95 gives better pitching-moment predictions on some configurations than the AP98 is the new model for wing-tail interference[17] incorporated into the AP98. This new model shows that for $\Phi = 0$ deg roll $C_{N_{T(V)}}$ is zero (and hence $C_{M_{T(V)}}$ is also zero) for the AP98 at $\alpha = 30$ deg and $M = 1.5$. However, the AP95 gives $C_{N_{T(V)}}$ of −1.18 and $C_{M_{T(V)}}$ of 9.07. If one adds this value to the AP98 results of Fig. 3d, one obtains the AP95 result. This discrepancy does not occur on all configurations. In general, the total C_N is predicted more accurately on all cases by the new $C_{N_{T(V)}}$ model of the AP98 than the older model of the AP95. However, about half of the pitching-moment predictions are better with the AP95 than the AP98. At this point in time, it is not clear whether this mixed success is caused by the wing-tail interference model or internal shock interactions moving the center of pressure forward as α increases. One effort planned for the future is to use a computational fluid dynamics (CFD) code to investigate this pitching-moment issue and hopefully improve upon the pitching-moment prediction so that all AP98 cases will be superior to AP95 predictions. However, at present, some pitching-moment predictions of the AP95 are better than those of the AP98. On the other hand, we have not found a case as of yet where the average accuracy levels of ±10% on C_A and C_N and 4% of body length for X_{CP} have been exceeded. By average is meant enough cases (αs and Ms) must be considered for a good statistical sample.

The next case considered is a six-fin projectile configuration (Fig. 4a). This case is chosen to illustrate how the AP98 can be used for six-fin cases although the code is only set up to allow either two- or four-fin options. The next version of the APC past the AP98 will, hopefully, allow the six-fin option. However, for the AP98 one has to use the code listing of individual aerodynamic components in conjunction with hand calculations to obtain the final set of aerodynamics. For example, the four-fin option is chosen for the AP98 computations. Then in the data tables all fin axial-force components are multiplied by 1.5, and this number replaces that of the fin axial force. Secondly, the fin normal-force components (wing-body and body-wing) are multiplied by a factor. We currently use a factor of 1.4 at AOA 0 deg, and this factor decreases to 1.3 at AOA of 30 deg and higher. Then the pitching moments are modified based on the new normal-force components for the fin and interference effects.

Figure 4b shows the C_A, $(C_{N_\alpha})_{\alpha \cong 0}$ and X_{CP} comparisons of the AP98 to ballistic range and full Navier–Stokes results taken from Ref. 36. Computations were made in the AP98 based on the "Wind Tunnel Model With No Boundary Layer Trip" option and at sea-level Reynolds number conditions. This option was selected, as opposed to a "Typical Flight Condition" option, because of the fact most models are machine-built vs production-made. A machine-built model means the model is usually smoother than a production weapon. Note, the comparison of the AP98 to the CFD computations of Ref. 36 are quite good, and both fall in the middle of the ballistic-range data. An exception to this is the axial-force coefficient at $M = 3.5$ and below where the ballistic-range data points show a much stronger increase in C_A with decreasing Mach number than does the AP98. It is not clear why this occurs but is possibly because of AOA effects in the ballistic-range data, which are not included in the AP98.

The next case considered is a wing-body-tail case with a low aspect-ratio wing and tested at the Naval Postgraduate School[37] at $M_\infty = 0.1$. The configuration is shown at the top of Fig. 5. Note that the model tested in the wind tunnel at the top of the figure is slightly different than that where calculations were performed with the AP95 and AP98. This slight configuration difference is due to the fact the APC cannot handle the detailed dorsal and wing geometry shown at the top of the figure. The configuration shown in the middle of Fig. 5 has the same aspect ratio, span, taper ratio, leading-edge sweep angle, and area of both the dorsal and tail as the actual model at the top of Fig. 5. Also, although not shown, the distance to the centroid of the planform areas is also held constant. Of course, the body is also the same between the two cases.

The only results given in Ref. 37 were for normal force. Experimental data and Missile DATCOM[38] results were both given in Ref. 37 for roll positions of $\Phi = 0$ and 45 deg. These results are

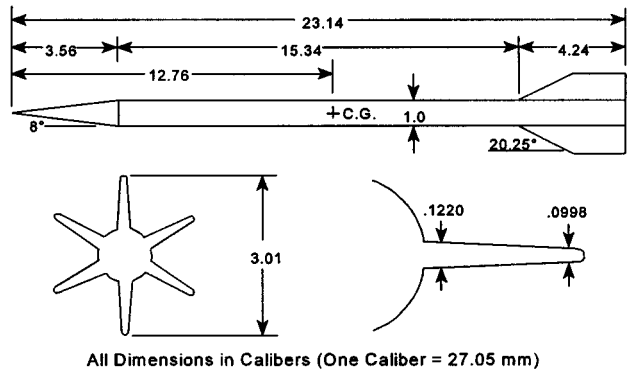

Fig. 4a Schematic of M829 projectile configuration (from Ref. 36).

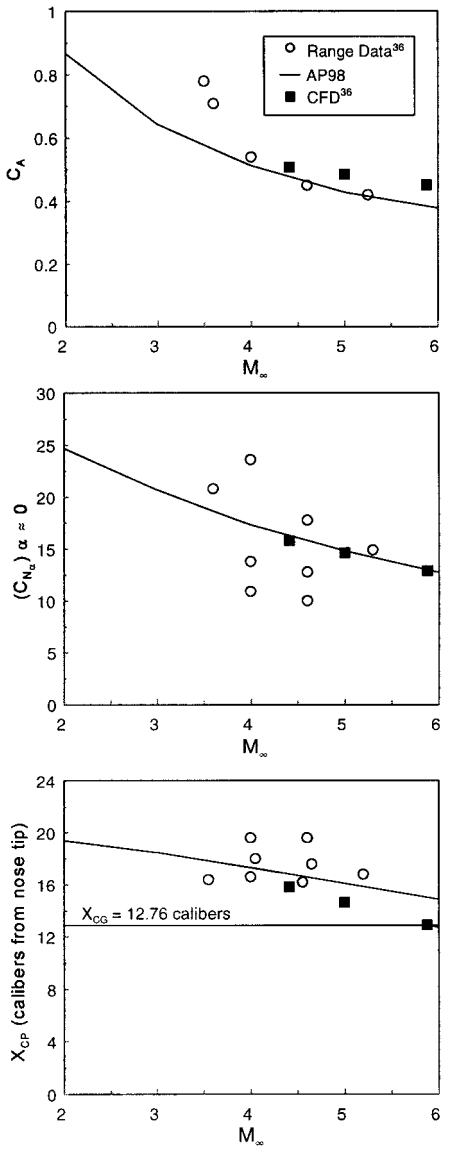

Fig. 4b Comparison of static aerodynamics between theory and experiment for Fig. 4a configuration.

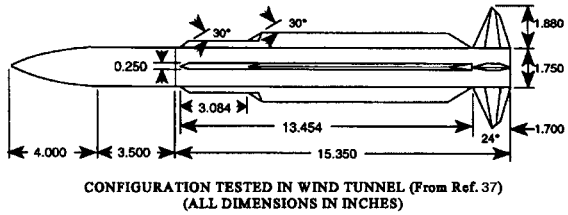

CONFIGURATION TESTED IN WIND TUNNEL (From Ref. 37)
(ALL DIMENSIONS IN INCHES)

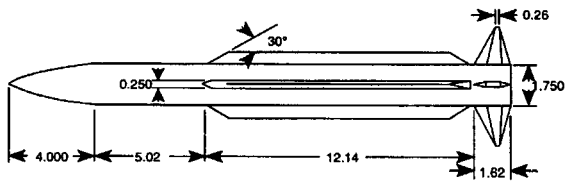

MODIFIED CONFIGURATION USED IN AEROPREDICTION COMPUTATIONS

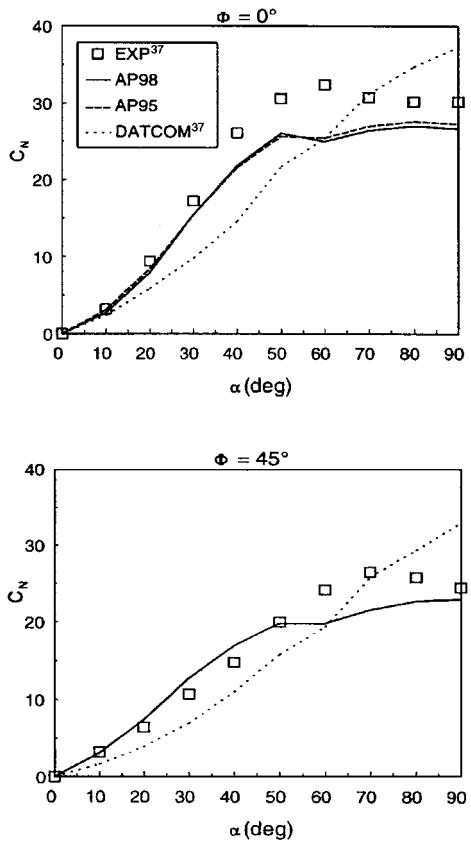

Fig. 5 Normal-force coefficient comparisons of body, dorsal, and tail ($M_\infty = 0.1$).

compared to the AP95 and AP98 at the bottom of Fig. 5 for $\Phi = 0$ deg and to the AP98 only for $\Phi = 45$ deg. Note that comparisons to data are reasonable and quite good except at AOA 40–70 deg. It is possible that wind-tunnel sting to model interference increased the experimental results in this range somewhat. Previous wind-tunnel studies[39,40] have concluded that the model sting can increase model normal-force loads by 10–20% in the high-AOA range. Both the AP95 and AP98 give slightly better comparisons to data than the Missile DATCOM[38] for this case. We suspected that the low-aspect-ratio lifting surfaces, which have a great deal of nonlinear lift, are the primary reason for the Missile DATCOM accuracy problems, particularly at $\Phi = 0$ deg.

The last axisymmetric body case considered is taken from Ref. 41 and is shown in Fig. 6. The model was about 22 calibers in length with a sharp nose of 2.25 calibers. The canards had an aspect and taper ratio of 2.0 and 0.3, respectively. Various tail fin spans were considered. This model was tested at Mach numbers 1.6–3.5 at AOA to about 18 to 20 deg. It had a boundary-layer trip present and was tested at an R_N/ft of 2.0×10^6. Reference 41 gave separate values of base axial-force coefficient, which were added to the axial-force values given in the reference to compare to the AP98 computations. To compare the experimental data to theory, Mach numbers of 2.5 and 3.5 are selected at roll angle 45 deg. Also, values of the tail-to-canard semispan of 0.47 and 1.25 are considered. Because $\Phi = 45$ deg roll is chosen, no AP95 computations will be shown. Figure 7 presents the comparison of theory to experiment for $b_t/b_c = 0.47$ and 1.25. Results are shown for C_A, C_N, and C_M.

As seen in Fig. 7, comparison of theory to experiment is quite acceptable and meets the average accuracy goal of ±10% on axial and normal force and ±4% of body length for center of pressure. The worst case error on pitching moment at $M = 2.5$ and $b_t/b_c = 1.25$ represents an error of less than 3% of the body length in terms of center of pressure. Also shown in Fig. 7 are M3HAX computations taken from Ref. 42 for the $b_t/b_c = 1.25$ case at $M = 2.5$. The C_A results for $\Phi = 0$ deg from Ref. 42 were assumed to apply to the $\Phi = 45$ deg case because no control deflections were assumed for this example. As seen in the Fig. 7, M3HAX gives reasonable comparison to data at $\Phi = 45$ deg. Reference 42 shows M3HAX giving improved comparisons to data at $\Phi = 0$ deg roll, compared to $\Phi = 45$ deg roll, particularly for normal-force and pitching-moment coefficients.

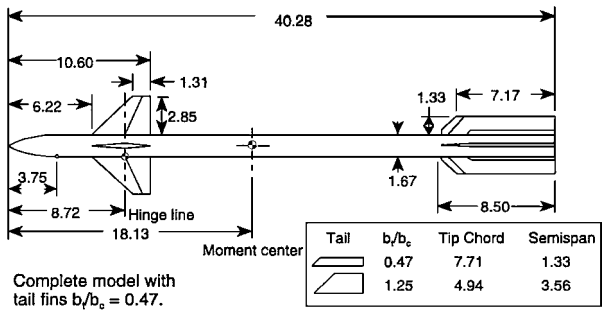

Fig. 6 Canard-body-tail configuration with varying tail span (all dimensions in inches).

The last three cases considered illustrate the new nonaxisymmetric body capability of the AP98. The first of these cases is based on the databases of Refs. 43 and 44, and the configurations considered are shown in Fig. 8a. Figure 8a illustrates elliptical cross-section configurations of ellipticity ratios of 2.0 at $\Phi = 0$ and 0.5 at $\Phi = 90$ deg. It also has squares at $\Phi = 0$ and diamonds at $\Phi = 45$ deg roll. Finally, triangular and inverted triangular cross-section shapes are also considered. All nonaxisymmetric body cases shown were run on the AP98 with an optimum value of the critical crossflow Mach number where transition from subcritical to supercritical conditions occur. This optimum value is not that critical for higher-Mach-number computations, but is very important to predict subsonic normal force accurately. The Fig. 8a configuration was tested to 24-deg AOA at $M_\infty = 1.98$ and 3.88 in Ref. 43. All bodies in Fig. 8a have the same cross-sectional area as the circle. The corner radii of the squares and triangles were very small, so a value of $k = 0$ was assumed in the computations. The elliptical shape 10-caliber body of Fig. 8a was tested later[44] at Mach numbers 0.6 to 2.0 and to AOA 56 deg. The case shown here will thus be the elliptical 10-caliber long body tests of Ref. 44, which go to 56-deg AOA, and the square and triangular tests of Ref. 43, which go only to 24-deg AOA. Not all results will be shown as the Refs. 43 and 44 databases were fairly extensive. Most of these results are shown in Ref. 21, however.

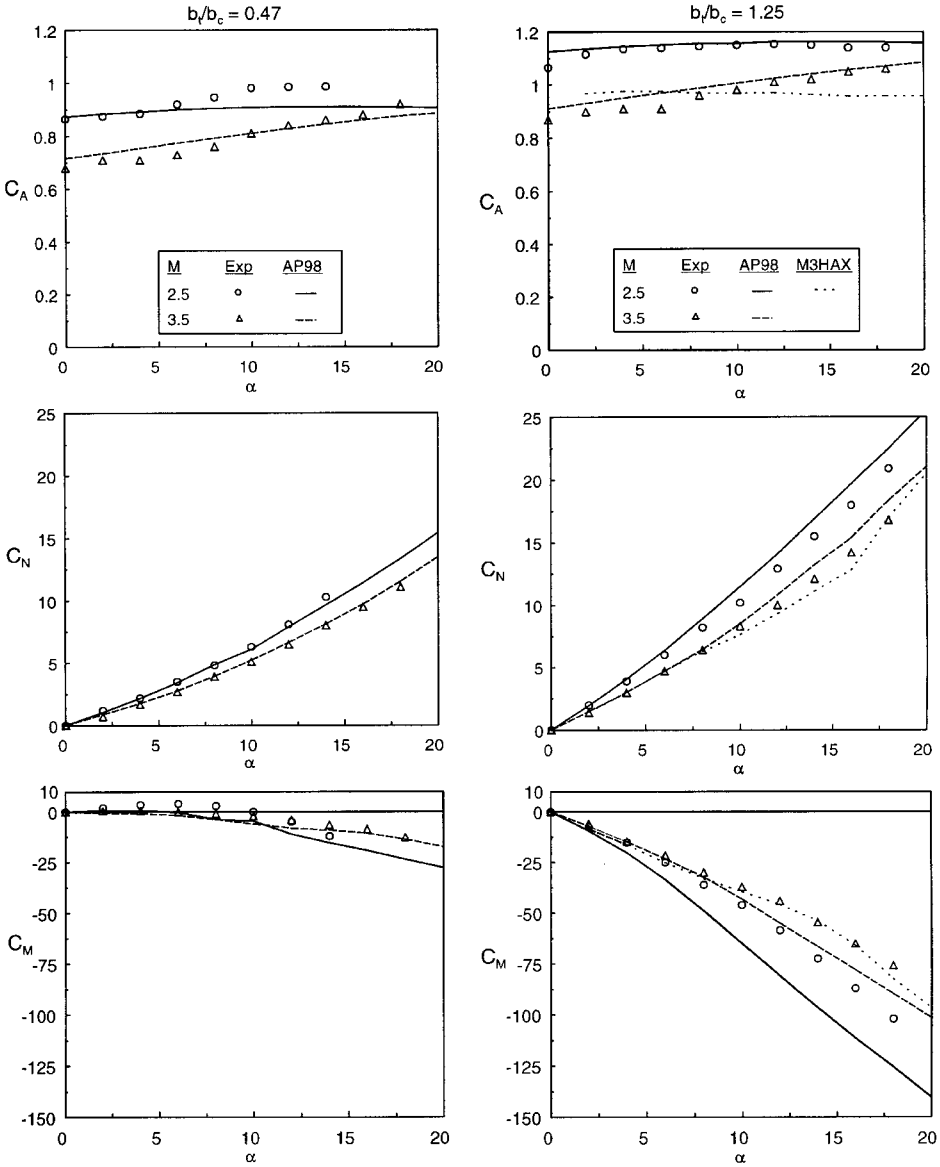

Fig. 7 Comparisons of theory and experiment[41] for configurations of Fig. 6 (Φ = 45 deg).

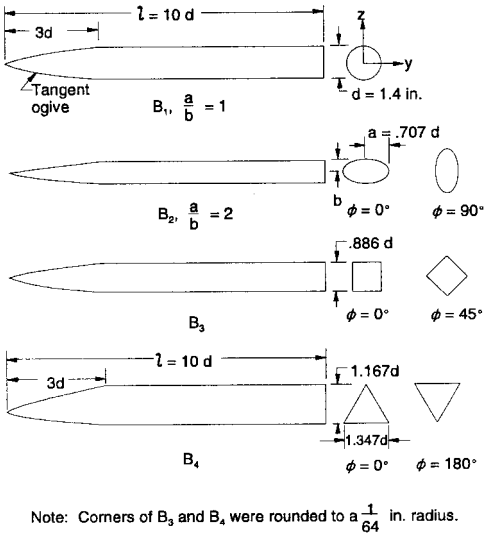

Fig. 8a Body-alone configurations with elliptical square, diamond, triangular, and inverted-triangular shapes.[43]

Figure 8b gives the elliptical body results for a Mach number of 2.0. Results shown are for ellipticity values of 0.5, 1.0, and 2.0 and are given in terms of normal- and axial-force coefficients and center of pressure. To get the ellipticity value of 0.5, configuration B_2 is simply rotated to the $\Phi = 90$ deg roll position as shown in Fig. 8b. Also, the axial-force coefficient does not include a base-drag component. In examining the Fig. 8b comparisons of theory and experiment, one can see the theory does a fairly good job of predicting the aerodynamics on the elliptical case. The normal-force and center-of-pressure predictions are quite encouraging as they are well within the average accuracy levels of ±10% and ±4% of body length, respectively. The axial-force prediction comparisons are not as good as desired. However, this could be because of measurement accuracy where it is difficult to get accurate axial-force measurements with a sting designed for measuring normal force at high AOA.

Theoretical and experimental results for the squares and triangles of Fig. 8a are given in Figs. 8c and 8d, respectively. Only the 10-caliber-long configuration results at $M = 1.98$ are shown. Here the results are given in terms of lift coefficient, lift-to-drag ratio, and center of pressure. In general, comparison of theory and experiment for the squares and diamonds is quite encouraging, although not as good as the circular cross-section shapes. The triangular-shaped

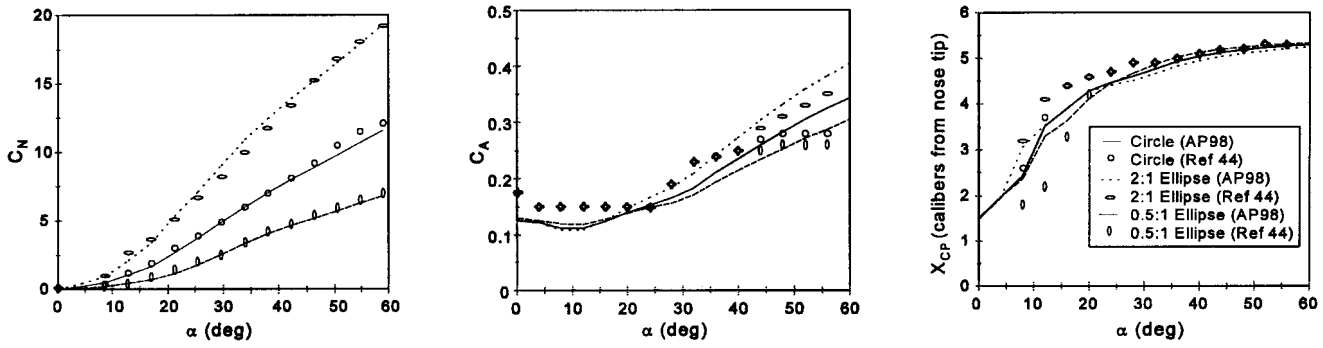

Normal-force coefficient **Axial-force coefficient** **Center of pressure**

Fig. 8b Aerodynamic data for 2:1 and 0.5:1 ellipses of Fig. 8a compared to circular body at $M = 20$.

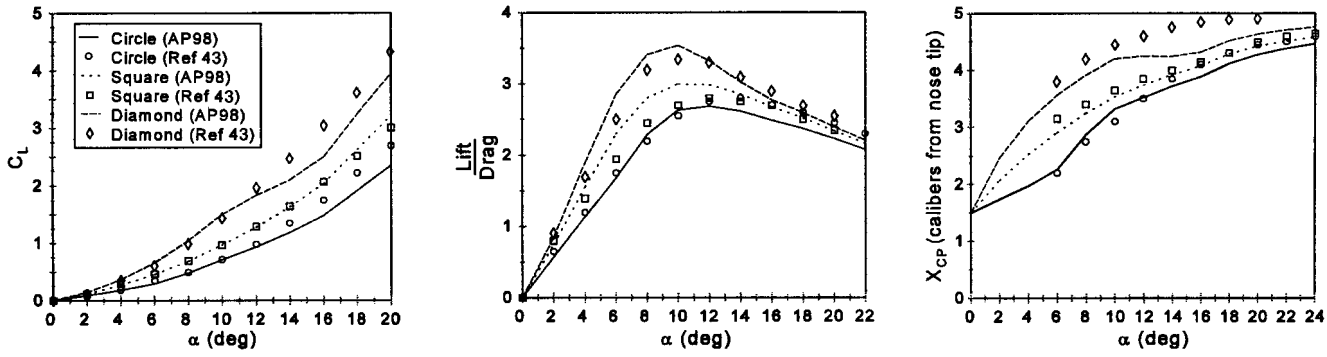

Lift coefficient **Lift-to-drag ratio** **Center of pressure**

Fig. 8c Aerodynamic data of squares ($k = 0.0$) and diamonds ($k = 0.0$) of Fig. 8a compared to circular body at $M = 1.98$ ($\ell/d = 10$).

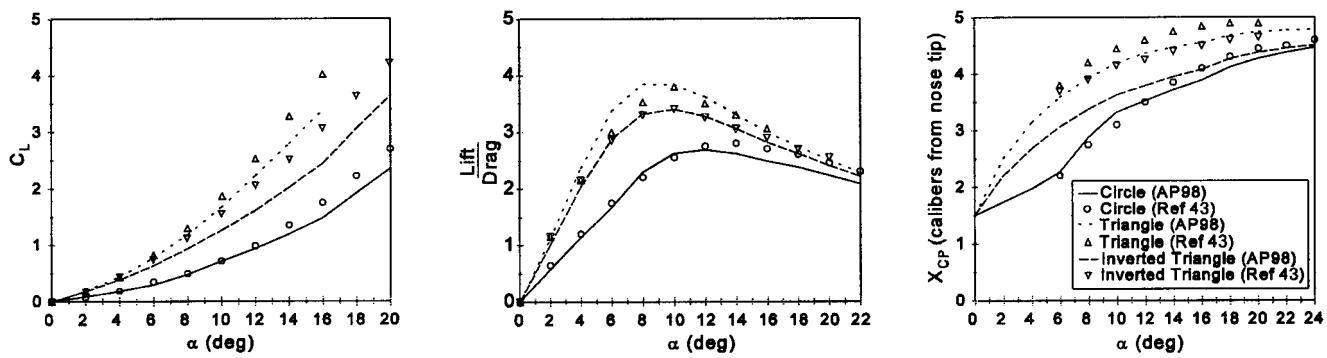

Lift coefficient **Lift-to-drag ratio** **Center of pressure**

Fig. 8d Aerodynamic data of triangles ($k = 0.0$) and inverted triangles ($k = 0.0$) of Fig. 8a compared to circular body at $M = 1.98$ ($\ell/d = 10$).

body predictions for lift coefficient tend to be somewhat low as AOA increases. However, this is to be expected because the values for the circular cylinder results are also low. Lift-to-drag ratio predictions are quite good, with the peak values being reasonably well predicted. The center-of-pressure prediction for the triangular shape is well within the ±4% of body length used as a criteria for axisymmetric bodies. However, the inverted triangle center-of-pressure predictions slightly exceed this value.

The next case considered is a 10-caliber wing-body and wing-body-tail case shown in Fig. 9a (Ref. 32). The body cross section is an ellipse with an $a/b = 2.0$, and the nose length is 3.0 calibers. Figures 9b and 9c present the normal-force and center-of-pressure comparisons of experiment and theory at $M = 0.6$ and 2.0 for the wing-body and wing-body-tail cases, respectively. Data for the wing-body-tail case at $M = 2.0$ were available only to $\alpha = 34$ deg, whereas all other cases have data to 60-deg AOA. As seen in Figs. 9b and 9c, theoretical predictions are quite good for center of pressure and fair to good for normal-force coefficient.

The last configuration shown (Fig. 10) is a waverider configuration taken from Ref. 45. Lift, drag, and pitching-moment

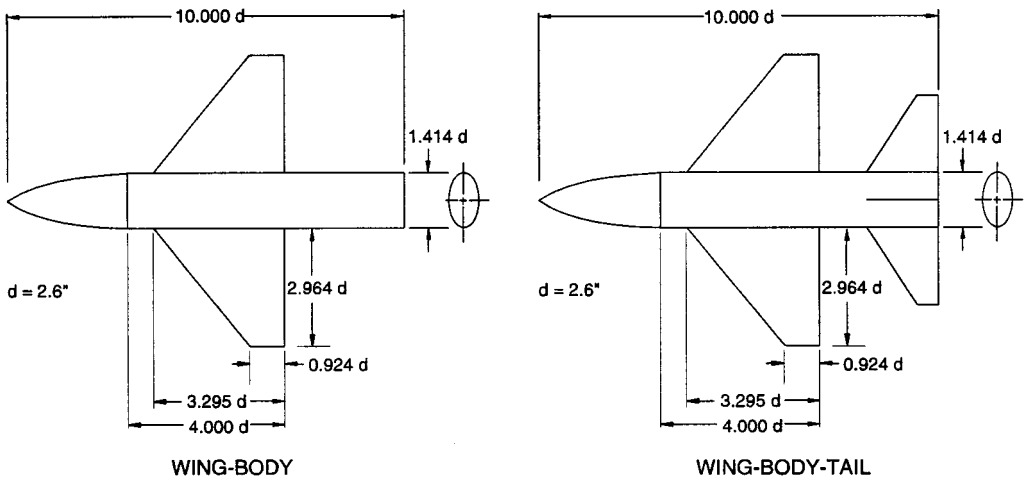

Fig. 9a Geometry of the wing-body and wing-body-tail configurations with 2:1 elliptical bodies (from Ref. 32).

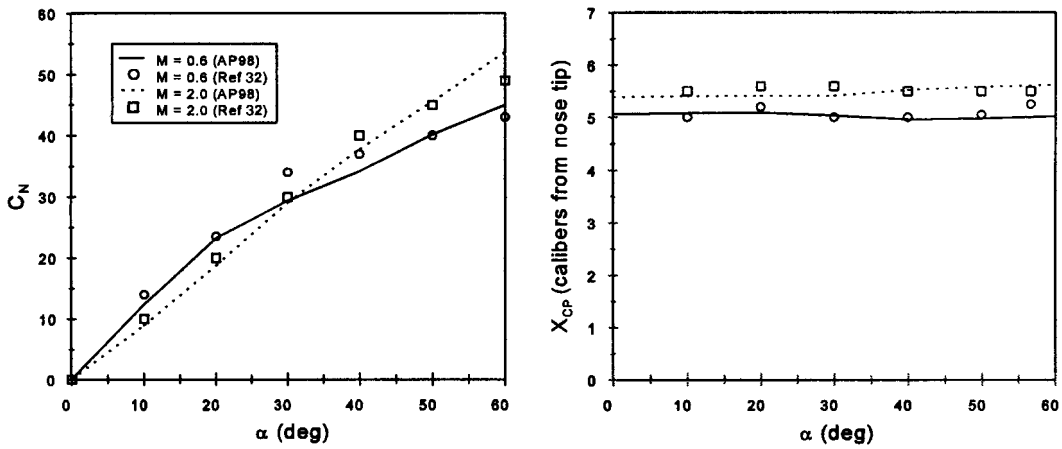

Normal-force coefficient **Center of pressure**

Fig. 9b Aerodynamic data for the wing-body configuration of Fig. 9a with a 2:1 elliptical cross-section body.

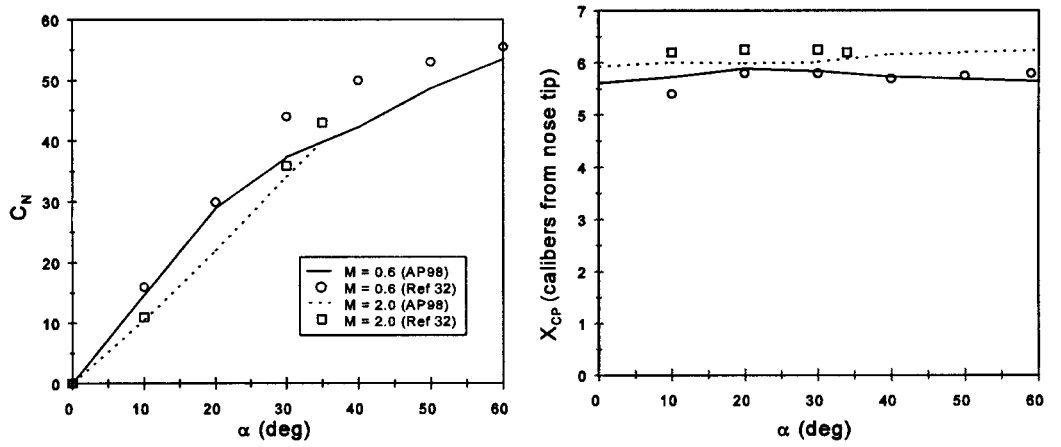

Normal-force coefficient **Center of pressure**

Fig. 9c Aerodynamic data for the wing-body-tail configuration of Fig. 9a with a 2:1 elliptical cross-section body.

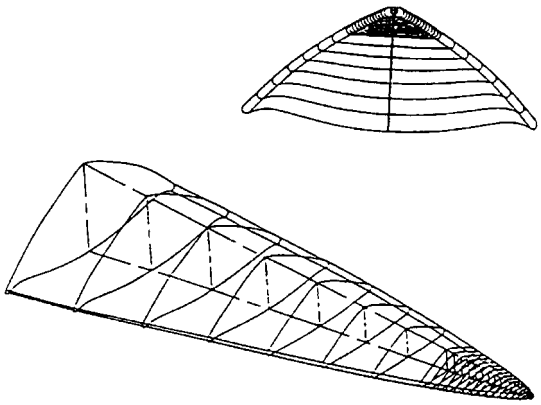

Fig. 10 Wire-frame geometry of the wave rider (from Ref. 45).

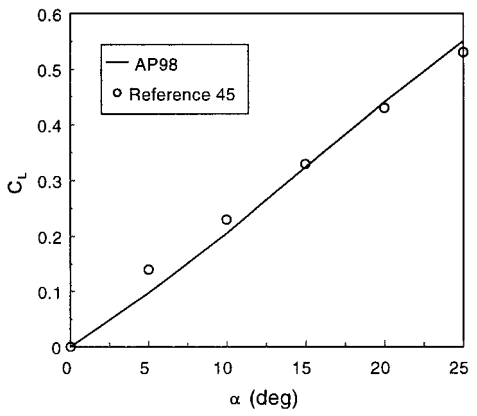

Lift coefficient

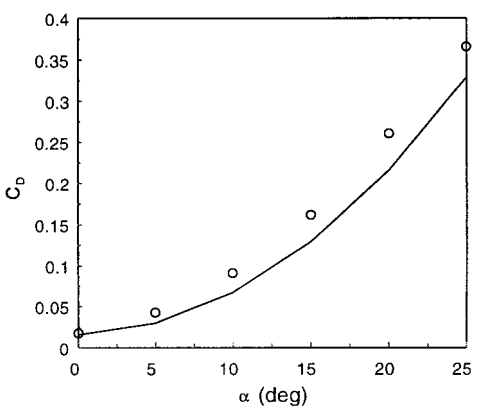

Axial-force coefficient

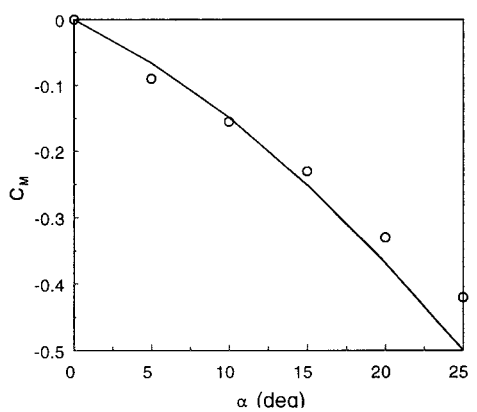

Moment coefficient

Fig. 11 Aerodynamic data for the Mach 14 wave rider of Fig. 10.

comparisons of theory and experiment at $M = 14.0$ to $\alpha = 25$ deg are shown in Fig. 11. Results are quite encouraging, even though this configuration does not quite fit the triangular shape, which has 60-deg angles in all corners. Note that these results are based on a 375-in.^{2} planform area.

No average accuracy assessment has been made as of yet for the nonaxisymmetric body configurations similar to that available for axisymmetric bodies. As more comparisons are made, this may become more feasible. At present, the average accuracy of the normal- and axial-force coefficients and center of pressure appear to be almost as good as the axisymmetric body if the configurations are similar to those of Fig. 2. However, when cases deviate substantially from the Fig. 2 options, average accuracy is expected to be degraded as well.

Future Opportunities

Future opportunities are placed in two categories. These categories are defined as major technology needs and value-added technology needs. The difference between the definition of major and value-added has to do with the cost to develop the technology and integrate it into the APC. Generally, before any new technology is developed, there needs to be a request from users and sponsor support to fund the technology development.

The NSWCDD APC has progressed to the point that it can compute planar aerodynamics with acceptable accuracy over the configuration and flight envelope of interest to most tactical weapons. The two remaining major technology needs are to account for aerodynamic effects of side jets and an accurate semi-empirical code for out-of-plane aerodynamics. The first problem requires a good generic wind-tunnel database, and this requirement is being marketed to the Ballistic Missile Defense Office. The latter need may be beyond the scope of a semi-empirical code because of the complex out-of-pitch plane aerodynamic nonlinearities and the fact that many of these nonlinearities are within the accuracy of the data.

This problem of accurate out-of-pitch plane aerodynamics is particularly true for induced roll. As a result, at NSWCDD, either wind-tunnel data or more accurate numerical codes have been used to predict out-of-plane aerodynamics. A less accurate (±25%) out-of-plane semi-empirical code may be feasible, but it is high risk.

There are several value-added technology needs that would enhance the capability of the APC significantly while being much less costly than the two major technology needs already described. Some of these include 1) using CFD to improve and validate the predictions outside the range of the databases (this is important because the databases are limited to Mach number less than 4.6 and AOA of 40 deg); 2) using a new NASA database for fine tuning r/s effects; 3) integrating the APC with other software models to form system engineering models; 4) modifying dynamic derivative calculations so flared vehicles can be handled; 5) including a six-fin option in the APC; 6) incorporating base bleed for projectile applications; 7) including nonlinear aerodynamics in the dynamic derivatives; and 8) incorporating methodology for internal shock interactions.

Over the history of the APC series (1972 to the present), significant advances have been made in semi-empirical aeroprediction methods. As seen in the opportunities list, much work still remains to be done.

Acknowledgments

The work described in this paper was supported through the Office of Naval Research (Dave Siegel) by the following programs: the Air Launched Weapons Program managed at the U.S. Naval Air Warfare Center, China Lake, California, by Tom Loftus and Craig Porter; and the Surface Weapons Systems Technology Program managed at the NSWCDD by Robin Staton and Gil Graff. Also, some support was provided by the Marine Corps Weaponry Technology Program managed at NSWCDD by Bob Stiegler. The authors express appreciation for support received in this work.

References

[1] Moore, F. G., "Body Alone Aerodynamics of Guided and Unguided Projectiles at Subsonic, Transonic, and Supersonic Mach Numbers," (AP72),

U.S. Naval Surface Warfare Center, Dahlgren Div., NWL TR-3796, Dahlgren, VA, Nov. 1972.

[2]Moore, F. G., and McKerley, C. W., "Aerodynamics of Guided and Unguided Weapons: Part I—Theory and Application," (AP74), U.S. Naval Surface Warfare Center, Dahlgren Div., NWL TR-3018, Dahlgren, VA, Dec. 1973.

[3]Moore, F. G., and Swanson, C., "Aerodynamics of Tactical Weapons to Mach Number 3 and Angle of Attack 15 Degrees: Part I—Theory and Application," (AP77), U.S. Naval Surface Warfare Center, Dahlgren Div., NSWCDL TR-3584, Dahlgren, VA, Feb. 1977.

[4]Devan, L., "Aerodynamics of Tactical Weapons to Mach Number 8 and Angle of Attack 180°: Part I, Theory and Application," (AP81), U.S. Naval Surface Warfare Center, Dahlgren Div., NSWC TR 80-346, Dahlgren, VA, Oct. 1980.

[5]Moore, F. G., Hymer, J., and McInville, R., "Improved Aeroprediction Code: Part I—Summary of New Methods and Comparison with Experiment," (AP93), U.S. Naval Surface Warfare Center, Dahlgren Div., NSWCDD TR-93/91, Dahlgren, VA, May 1993.

[6]Moore, F. G., McInville, R. M., and Hymer, T. C., "The 1995 Version of the NSWC Aeroprediction Code: Part I—Summary of New Theoretical Methodology," (AP95), U.S. Naval Surface Warfare Center, Dahlgren Div., NSWCDD/TR-94/379, Dahlgren, VA, Feb. 1995.

[7]Moore, F. G., McInville, R. M., and Hymer, T. C., "The 1998 Version of the NSWC Aeroprediction Code: Part I—Summary of New Theoretical Methodology," (AP98), U.S. Naval Surface Warfare Center, Dahlgren Div., NSWCDD/TR-98/1, Dahlgren, VA, April 1998.

[8]Graff, G., and Moore, F. G., "Empirical Method for Predicting the Magnus Characteristics of Spinning Shells," *AIAA Journal*, Vol. 15, No. 10, 1977, pp. 1379, 1380.

[9]DeJarnette, F. R., Ford, C. P., and Young, D. E., "Calculation of Pressures on Bodies at Low Angles of Attack in Supersonic Flow," *Journal of Spacecraft and Rockets*, Vol. 17, No. 6, 1980, pp. 529–536.

[10]Chaussee, D. S., "Improved Transonic Nose Drag Estimates for the NSWC Missile Aerodynamic Computer Program," Nielsen Engineering CR Prepared for NSWCDD, as NSWC/DL TR-3830, Dahlgren, VA, April 1978.

[11]Moore, F. G., Armistead, M., Rowles, S., and DeJarnette, F. R., "Second-Order Shock Expansion Theory Extended to Include Real Gas Effects," U.S. Naval Surface Warfare Center, Dahlgren Div., NAVSWC TR 90-683, Dahlgren, VA, Feb. 1992.

[12]Moore, F. G., Hymer, T., and Devan, L., "New Methods for Predicting Nonlinear Lift, Center of Pressure, and Pitching Moment on Missile Configurations," U.S. Naval Surface Warfare Center, Dahlgren Div., NSWCDD/TR-92/217, Dahlgren, VA, July 1992.

[13]McInville, R. M., and Moore, F. G., "Incorporation of Boundary Layer Heating Predictive Methodology into the NAVSWC Aeroprediction Code," U.S. Naval Surface Warfare Center, Dahlgren Div., NSWCDD TR-93/29, Dahlgren, VA, April 1993.

[14]Moore, F. G., Wilcox, F., and Hymer, T., "Improved Empirical Model for Base Drag Prediction on Missile Configurations Based on New Wind Tunnel Data," U.S. Naval Surface Warfare Center, Dahlgren Div., NSWCDD TR-92/509, Dahlgren, VA, Oct. 1992.

[15]Moore, F. G., and McInville, R. M., "A New Method for Calculating Wing Alone Aerodynamics to Angle of Attack 180 Degrees," U.S. Naval Surface Warfare Center, Dahlgren Div., NSWCDD/TR-94/3, Dahlgren, VA, March 1994.

[16]Moore, F. G., and McInville, R. M., "Extension of the NSWCDD Aeroprediction Code to the Roll Position of 45 Degrees," U.S. Naval Surface Warfare Center, Dahlgren Div., NSWCDD/TR-95/160, Dahlgren, VA, Dec. 1995.

[17]Moore, F. G., and McInville, R. M., "A New Semiempirical Model for Wing-Tail Interference," AIAA Paper 96-3393, July 1996.

[18]McInville, R. M., Moore, F. G., and Housh, C., "Nonlinear Structural Load Distribution Methodology for the Aeroprediction Code," U.S. Naval Surface Warfare Center, Dahlgren Div., NSWCDD/TR-96/133, Dahlgren, VA, Sept. 1996.

[19]Moore, F. G., and Hymer, T. C., "An Improved Method for Predicting Axial Force at High Angle of Attack," U.S. Naval Surface Warfare Center, Dahlgren Div., NSWCDD/TR-96/240, Dahlgren, VA, Feb. 1997.

[20]Hymer, T. C., Downs, C., and Moore, F. G., "A Interactive, User-Friendly, Personal Computer Version of the Aeroprediction Code," U.S. Naval Surface Warfare Center, Dahlgren Div., NSWCDD/TR-94/107, Dahlgren, VA, June 1994.

[21]Moore, F. G., and McInville, R. M., "An Improved Semiempirical Method for Calculating Aerodynamics of Missiles with Noncircular Bodies," U.S. Naval Surface Warfare Center, Dahlgren Div., NSWCDD/TR-97/20, Dahlgren, VA, June 1997.

[22]Van Dyke, M. D., "First and Second-Order Theory of Supersonic Flow Past Bodies of Revolution," *Journal of Aeronautical Sciences*, Vol. 18, No. 3, 1951, pp. 161–179.

[23]Syvertson, C. A., and Dennis, D. H., "A Second-Order Shock-Expansion Method Applicable to Bodies of Revolution Near Zero Lift," NACA TR-1323, 1957.

[24]Wu, J. M., and Aoyoma, K., "Pressure Distributions for Axisymmetric Bodies with Discontinuous Curvature in Transonic Flow," U.S. Army Missile Command, TR RD-TR-70-25, Huntsville, AL, Nov. 1970.

[25]Van Driest, E. R., "Turbulent Boundary Layers in Compressible Fluids," *Journal of the Aeronautical Sciences*, Vol. 18, No. 3, 1951, pp. 145–160, 216.

[26]Tsien, H. S., "Supersonic Flow over an Inclined Body of Revolution," *Journal of the Aeronautical Sciences*, Vol. 5, No. 12, 1938, pp. 480–483.

[27]Pitts, W. C., Nielson, J. N., and Kaatari, G. E., "Lift and Center of Pressure of Wing-Body-Tail Combinations at Subsonic, Transonic, and Supersonic Speeds," NACA TR-1307, 1957.

[28]Allen, J. H., and Perkins, E. W., "Characteristics of Flow over Inclined Bodies of Revolution," NACA RMA 50L07, March 1951.

[29]NASA Langley Research Center Tri-Service Missile Data Base, Transmitted from NASA/Langley Research Center, Jerry M. Allen to Naval Surface Warfare Center, Dahlgren, VA, Nov. 1991 (formal documentation of database in process).

[30]Stallings, R. L., Jr., and Lamb, M., "Wing-Alone Aerodynamic Characteristics for High Angles of Attack at Supersonic Speeds," NASA TP-1989, July 1981.

[31]Baker, W. B., Jr., "Static Aerodynamic Characteristics of a Series of Generalized Slender Bodies with and Without Fins at Mach Numbers from 0.6 to 3.0 and Angles of Attack from 0 to 180°," Arnold Engineering Development Center, AEDC TR-75-124, Vols. 1 and 2, Tullahoma, TN, May 1976.

[32]Jorgensen, L. H., "A Method for Estimating Static Aerodynamic Characteristics for Slender Bodies of Circular and Noncircular Cross Section Alone and with Lifting Surfaces at Angles of Attack from 0° to 90°," NASA TN-D-7228, 1973.

[33]Nelson, H. F., "Wing-Body Interference Lift for Supersonic Missiles with Elliptical Cross-Section Fuselages," *Journal of Spacecraft and Rockets*, Vol. 26, No. 5, 1989, pp. 322–329.

[34]Est, B. E., and Nelson, H. F., "Wing-Body Carryover and Fin Center of Pressure for Missiles with Noncircular Fuselage Cross Sections," AIAA Paper 91-2856, Aug. 1991.

[35]Monta, W. J., "Supersonic Aerodynamic Characteristics of a Sparrow III Type Missile Model with Wing Controls and Comparison with Existing Tail-Control Results," NASA TP-1078, Nov. 1977.

[36]Guidos, B. J., "Static Aerodynamics CFD Analysis for 120 MM Hypersonic KE Projectile Design," U.S. Army Research Lab., ARL-MR-84, Aberdeen Proving Ground, MD, Sept. 1984.

[37]Howard, R. M., and Dunn, A., "Missile Loads at High Angles of Attack," *Journal of Spacecraft and Rockets*, Vol. 28, No. 1, 1991, pp. 124, 125.

[38]Vukelich, S. R., and Jenkins, J. E., "Missile DATCOM: Aerodynamic Prediction on Conventional Missiles Using Component Build-Up Techniques," AIAA Paper 84-0388, Jan. 1984.

[39]Deitz, W. E., Jr., and Altstatt, M. C., "Experimental Investigation of Support Interference on an Ogive Cylinder at High Incidence," *Journal of Spacecraft and Rockets*, Vol. 16, No. 2, 1979, pp. 67, 68.

[40]Canning, T. N., and Nielsen, J. N., "Experimental Study of the Influence of Supports on the Aerodynamic Loads on a Ogive Cylinder at High Angles of Attack," AIAA Paper 81-0007, Jan. 1981.

[41]Blair, A. B., Jr., Allen, J. M., and Hernandez, G., "Effect of Tail-Fin Span on Stability and Control Characteristics of a Canard Controlled Missile at Supersonic Mach Numbers," NASA TP-2157, June 1983.

[42]Lesieutre, D. J., Love, J. F., and Dillenius, M. F., "M3HAX Aerodynamic Analysis for Finned Vehicles with Axisymmetric Bodies," NEAR, Inc., NEAR TR 493-D, Mountain View, CA, Feb. 1996.

[43]Jorgensen, L. H., "Inclined Bodies of Various Cross Sections at Supersonic Speeds," NASA Memo 10-3-58A, 1958.

[44]Jorgensen, L. H., and Nelson, E. R., "Experimental Aerodynamic Characteristics for Bodies of Elliptic Cross Section at Angles of Attack from 0° to 58° and Mach Numbers from 0.6 to 2.0," NASA TM-X-3129, 1975.

[45]Gillum, M. J., and Lewis, M. J., "Analysis of Experimental Results on a Mach 14 Waverider with Blunt Leading Edges," AIAA Paper 96-0812, Jan. 1996.

R. M. Cummings
Associate Editor